Theor Appl Climatol (2013) 111:275–284
DOI 10.1007/s00704-012-0663-5

ORIGINAL PAPER

Surface atmospheric circulation patterns and associated minimum temperatures in the Maipo and Casablanca valleys, central Chile

Carlo Montes · Ricardo C. Muñoz · Jorge F. Perez-Quezada

Received: 14 February 2012 / Accepted: 18 April 2012 / Published online: 8 May 2012

Abstract This paper analyzes the influence of circulation anomalies on the magnitude of minimum air temperature (T_{min}) at a daily scale in two important agricultural valleys of Chile (Maipo and Casablanca) during the period 2001–2007. A statistical classification of synoptic fields was performed, resulting in eight circulation patterns (CPs, 84 % of explained variance). The corresponding anomalies of T_{min} (AT_{min}) of each CP were analyzed in order to understand their synoptic-scale forcing mechanisms. Results showed a direct association between AT_{min} and the synoptic structure. The average weakening in sea level pressure (SLP) yields positive AT_{min}, while negative AT_{min} is associated with a strengthening in SLP. In the latter case, it was also found that a synoptic structure (10.2 % of frequency) corresponding to a migratory high-pressure system passing eastward across the Andes led to the lowest AT_{min} and a higher probability of frost in both valleys (22 % on average) in winter and springtime.

C. Montes (✉) · R. C. Muñoz
Departamento de Geofísica, Universidad de Chile,
Av. Blanco Encalada 2002,
Santiago, Chile
e-mail: ccmontesv@gmail.com

J. F. Perez-Quezada
Departamento de Ciencias Ambientales y Recursos Naturales Renovables, Universidad de Chile,
Casilla 1004,
Santiago, Chile

Present Address:
C. Montes
Centro de Estudios Avanzados en Zonas Aridas (CEAZA),
Casilla 599,
La Serena, Chile

1 Introduction

Minimum air temperature (T_{min}) is one of the most important environmental variables in agriculture. Most deciduous fruit trees require a certain period of low temperatures to break dormancy (Faust et al. 1997), while low temperatures during the growing season can limit quality, phenological development, yields, or geographical distribution of agricultural species (Ashworth 1992; Jackson and Lombard 1993; Rodrigo 2000). Furthermore, frosts are major climatic hazards in agriculture, being responsible for yield losses and damage to vegetable crops, orchard trees, or vineyards (Rodrigo 2000). Early-bloom species can be strongly affected by frost episodes in springtime, with important economical impacts (Snyder and de Melo-Abreu 2005).

Local and regional processes at different geographic scales determine T_{min} variability. Microclimatic factors that modify the surface energy balance and the nocturnal boundary layer structure, such as air and surface water content, atmospheric stability, or microsite exposure, can enhance or reduce the longwave radiative loss from a vegetated surface, thus regulating surface cooling (Oke 1987; Cellier 1993; Jordan and Smith 1995; Rossi et al. 2002). Along with these factors, the topographical configuration of complex terrain can drive the formation of confined structures of air colder than its surroundings (Whiteman et al. 2001). These lowland cold air accumulations may be altered by along-valley wind systems during clear and undisturbed nighttime periods (Clements et al. 2003) when the valley geometry allows the development of downslope along-valley flow (Vosper and Brown 2008). Large-scale atmospheric circulations interact with the above-mentioned local features to produce a given surface temperature climatology. Strong synoptic flows can erode the surface shallow air pools (Zhong et al. 2003) or modify surface temperatures by advection of colder

or warmer air from different latitudes (Zängl 2005). Also, high-pressure systems are commonly associated with cloudless skies and a drier atmosphere, which enhance the longwave radiative loss from the land surface and result in a larger nocturnal cooling (e.g., Zhong et al. 2001).

Several studies have been conducted to analyze the influence of synoptic structures on extreme surface air temperatures. For South America, these studies have focused mostly on cold air episodic events in the eastern part of the continent (e.g., Vera and Vigliarolo 2000; Müller 2007, 2010; Rusticucci 2012). For instance, Marengo et al. (1997) described synoptic-scale cold air incursions, so-called cold surges, as an important phenomenon responsible for strong frost episodes in eastern South America, causing extended agricultural damage. In these cases, as also explained by Garreaud (2000, 2001), cold advection produced by a southerly synoptic flow resulting from a strong surface pressure gradient in southern South America drives a low-level wind that brings cold air from polar latitudes to the continent. High-pressure anomalies and southerly surface circulation were found as the most important large-scale factors linked to persistent low temperatures and frost episodes over regions of southeastern South America (Müller et al. 2003, 2005; Müller and Berri 2007, 2012).

Considering the lack of studies on T_{min} for western extratropical South America, the present work aims at understanding the synoptic-scale forcing mechanisms of T_{min} for two important Chilean agricultural zones: the Maipo and Casablanca valleys. Our working hypothesis is that for the particular zone considered, local factors, such as topography and surface energy balance, may be superimposed on the large-scale configuration and dynamics to explain the local T_{min} climatology. A statistical classification of sea level pressure (SLP) patterns was performed in order to characterize the dominant regional circulation anomalies. Then, the minimum temperature anomalies (AT_{min}) and frost probabilities are associated with the different circulation patterns (CPs). The current study is motivated by the importance of the two selected valleys as areas of agriculture production (see "Section 2.1") and the relevance of T_{min} as an environmental constraint for successful cultivation of agricultural species. Results presented below account for the direct influence of synoptic systems as large-scale factors on T_{min}, which is highly relevant for agricultural activities.

2 Data and methodology

2.1 Study area and data

The Maipo and Casablanca valleys are located in central Chile (Fig. 1). This region is characterized by a complex topography and by the presence of two mountain systems that bound a central depression: the Andes Cordillera to the east and the Coastal mountain range to the west. Agriculture, which is carried out mainly at the bottom of the valleys, represents one of the main economical activities. The Maipo Valley, with an agricultural surface of ~2,500 km^2, is characterized by the cultivation of fruits trees, horticultural crops, and viticulture. In the Casablanca Valley (~220 km^2), which is located on the Coastal range, grapevine cultivation is the most important agricultural activity, being recognized as one of most suitable zones for producing white wines in Chile (Montes et al. 2012). The regional climate is characterized by annual rainfall (~400 mm $year^{-1}$ in a regional average) concentrated in winter months (Falvey and Garreaud 2007) and by an interannual variability highly regulated by the El Niño-Southern Oscillation phenomenon, showing above (below) than normal amounts during El Niño (La Niña) years (Montecinos and Aceituno 2003). The synoptic variability is larger in winter months due to the more frequent passage of extratropical frontal systems across central Chile (Garreaud and Aceituno 2007), and the influence of the subtropical anticyclone of the southeastern Pacific induces a large prevalence of clear-sky days and weak synoptic pressure gradients over the region. Daily temperatures decrease from inland to coastal zones (e.g., Montes et al. 2012) and springtime months have been reported as those with higher threat of frost for agricultural species.

Data from three weather stations located in the valleys of Maipo (Codigua and La Platina stations, 33.76°S 71.32°W, and 33.57°S 70.62°W, respectively) and Casablanca (Casablanca station, 33.32°S 71.44°W) were analyzed (Fig. 1). Daily T_{min} measurements were considered for the available period, 1 January 2001 to 31 December 2007. It should be noted that although the use of a larger dataset could allow for a more detailed description of the within-valley T_{min} variability, the large-scale approach of this study and the valley's spatial dimensions suggest that the three selected stations are sufficient to represent the main T_{min} features associated to the synoptic-scale analysis. In order to perform the synoptic classification, daily fields of SLP and wind components for the same period (2001–2007) were obtained from the European Centre for Medium-Range Weather Forecast reanalysis (ECMWF 2010) (horizontal resolution of 1.0° latitude by 1.0° longitude). The domain chosen extends from the Equator to 60°S latitude and from 40°W to 100°W longitude, which allowed us to include the main large-scale factors influencing the atmospheric circulation over the study area, such as the Andes Cordillera and the adjacent Pacific Ocean. Prior to the analysis, anomalies of T_{min}, SLP, zonal and meridional wind components for the time series, and grid points were obtained by removing the annual cycle after subtracting from each daily

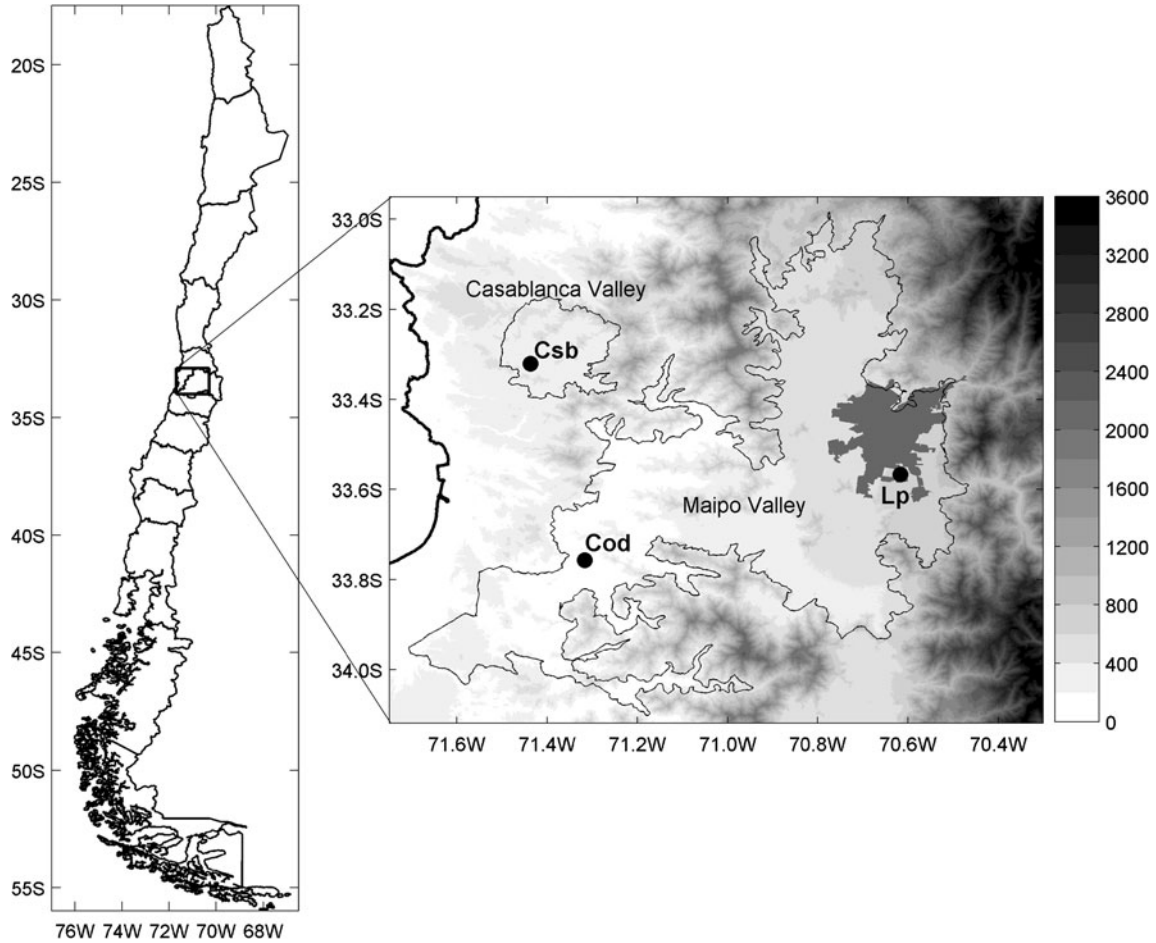

Fig. 1 Location and topography of the study area, and position of the weather stations (*black circles*). *Csb* Casablanca, *Cod* Codigua, *Lp* La Platina. *Bar* in meters above sea level. *Thin lines* delimit the Maipo and Casablanca valleys and thick lines are administrative divisions (omitted in topographic map for a better appreciation). The *darker polygon* in the Maipo Valley shows the city of Santiago

value the corresponding long-term 2001–2007 average for each day.

2.2 Statistical classification procedure

A synoptic classification of SLP fields was performed using an eigenvector-based method (e.g., Romero et al. 1999; Jiménez et al. 2009). First, a Principal Components Analysis (PCA) was applied to the covariance matrix of SLP anomalies to retain the main modes of variation according to the Scree test of Cattell (1966), which considers the analysis of the relationship between the explained variance (or the eigenvalue magnitude) and the component number to select the modes to retain. In order to conserve the orthogonal structure of the PCA factor loadings, the obtained components were rotated using the Varimax method (Richman 1986). Second, a two-step Cluster Analysis (CA) was applied to the previously selected modes of variation. In the first step, a hierarchical CA was performed using the Euclidean Distance as a measure of similarity, which for days a and b is defined as (Wilks 2006):

$$d_{ab} = \frac{1}{N_{ab}} \left[\sum_{i=1}^{N_{ab}} (SLP_{ai} - SLP_{bi})^2 \right]^{1/2}, \quad (1)$$

where d_{ab} is the average Euclidean Distance calculated over the N_{ab} points for days a and b. After calculating the similarity coefficient, the Ward's hierarchical method (Ward 1963) was used as the grouping algorithm. Similar to the PCA modes, the number of clusters was selected by plotting the distance between merged clusters and the number of formed clusters at the respective stage. The change in the slope of this relationship was used as an indicator of the appropriate number of clusters to be retained (see Wilks 2006 for method's description). As a second step of the CA, the nonhierarchical k means analysis (Anderberg 1973) was performed for the number of clusters previously found. As a way to ensure that the analysis was centered on the study area, the procedure was performed

over the geographical window defined by 60°W–90°W longitude and 20°S–45°S latitude (Fig. 2). However, for a better appreciation of the synoptic structures, the resulting pressure patterns were displayed over the full domain of the SLP fields. After the statistical classification, composites of wind vector fields were displayed and analyzed from the corresponding u and v components, and the AT_{min} of the corresponding days of each SLP group (or CP) were analyzed for the three weather stations. Finally, a one-way analysis of variance (ANOVA) was undertaken to compare the mean AT_{min} of each CP for individual stations, and the significant differences ($\alpha = 0.05$) were separated with a one-way Tukey's multiple comparison test.

3 Results and discussion

Figure 3 shows the monthly distributions of daily T_{min} for the three weather stations. As monthly averages for 2001–2007, the lower values are reached in June (2.8 °C, 2.7 °C, and 4.0 °C for Casablanca, La Platina, and Codigua, respectively), whereas the maximum values are reached in December (9.4 °C, 12.3 °C, and 11.9 °C, respectively). Temperatures below and near 0 °C occur from April to September. However, a large monthly dispersion is observed for the whole annual cycle, indicating an important interdaily variability that is larger in the cold season. A clear difference in T_{min} appears for the three weather stations. For the entire period, Casablanca shows the lowest mean annual T_{min} (6.7 °C), followed by La Platina (7.7 °C), and Codigua (8.8 °C). Several factors that influence the local behavior of air temperature may explain the observed differences between the three zones, e.g., regional elements, such as the sea proximity, the influence of the marine boundary layer in the coastal zone, or the topographic configuration (Montes 2010), but these issues are not addressed in this work.

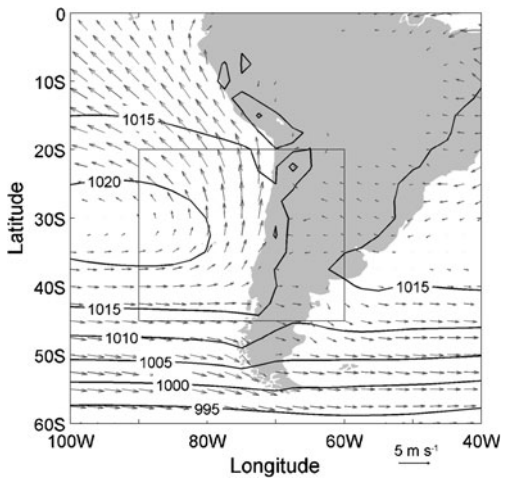

Fig. 2 Average composite of sea level pressure (hectopascals) and wind vectors (meter per second; reference vector at the bottom) for period 2001–2007. Only wind vectors with magnitude higher than 1 m s^{-1} are shown. *Interior rectangle* corresponds to the geographical window used for the statistical classification

The first step of the statistical procedure was to apply the PCA to the selected geographical window (see Fig. 2) to calculate the most relevant modes of variation of SLP and then to perform the classification procedure. The explained variance of the first ten PCA modes is shown in Fig. 4a. The slope break after the third principal component suggests that three modes (explaining 84 % of the total variance) should be retained for the CA procedure. Figure 4b shows the distance between clusters sequentially merged versus the number of formed groups. A large increase in the distance between two merged clusters is used as an indicator of when the algorithm should be stopped, since at this point, two very different clusters are merged (e.g., Jiménez et al. 2008). Figure 4b shows an increase in the Euclidean Distance at the fourth and eighth steps, suggesting an adequate number of five or nine groups of PCA to be retained. The exploration of the obtained CPs showed that the selection of five clusters excluded some relevant synoptic patterns, and very similar SLP structures appeared after the eighth cluster, so that a total of eight clusters have been selected for the subsequent analysis.

3.1 Surface circulation patterns (CPs)

The composites of SLP anomalies and wind vectors for the eight groups obtained with the classification procedure are displayed in Fig. 5. Their mean monthly relative frequency is presented in Fig. 6. The physical significance of the CPs associated with each cluster can be assessed by considering their SLP structure, seasonal frequency, and pressure disturbance's strength and position, as discussed next. Also, for a better interpretation of the mean CPs, the average field of SLP and wind vectors for the entire period 2001–2007 is shown in Fig. 2.

CP1 (Fig. 5a) is characterized by a deep field of positive SLP anomalies centered to the southwest of the continent over the Southeastern Pacific (n[1]=170, 6.6 % of total SLP fields), corresponding to a strengthening of the South Pacific anticyclone (shown as a climatological feature in Fig. 2) prevailing in the cold season and springtime (Fig. 6). The reinforced southerly surface circulation over the western part of the continent can bring colder-than-average air from higher latitudes to practically the whole Chilean territory. In addition, this synoptic structure could be related to a higher frequency of clear sky conditions, given the associated high pressures (e.g., Trigo et al. 2002). With a similar structure to CP1, CP2 (n=439, 17.2 %) consists of a high-pressure configuration located closer to the continent, but with a relative southward displacement and lower SLP anomalies. CP1 and CP2 show an opposite seasonal occurrence, CP2 being more frequent in

[1] Indicates the number of SLP fields forming each CP.

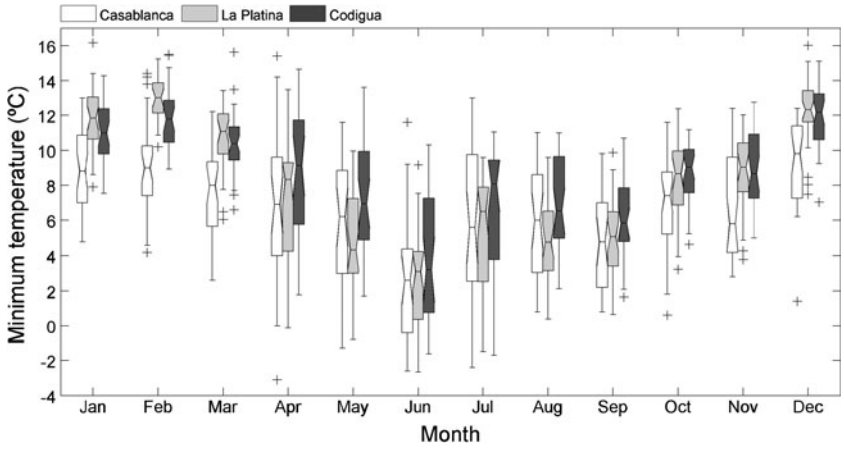

Fig. 3 *Boxplots* of monthly distributions of daily minimum temperature (2001–2007) in Casablanca, La Platina, and Codigua. For each box, the *central mark* shows the median, the *edges* of the box are the 25th and 75th percentiles, the *lines* extend to the most extreme values not considered outliers, and outliers are plotted individually (*plus sign*)

the warm season (Fig. 6). The circulation features found in these two patterns resemble the average conditions, also showing the seasonal behavior of the South Pacific anticyclone (e.g., Compagnucci and Salles 1997). In addition, the larger number of elements of CP2 shows the prevalence of the high pressures in the summer, which limits and regulates the synoptic variability in Chile during these months (Satymurty et al. 1998; Garreaud and Aceituno 2007).

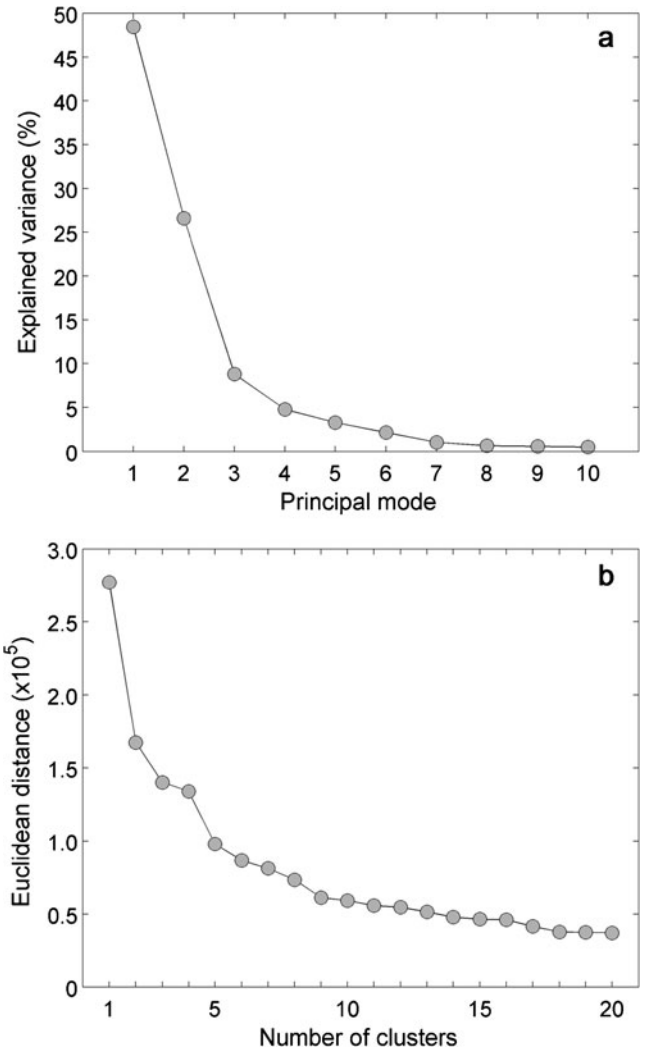

Fig. 4 **a** Explained variance by the ten leading PCA modes of SLP (Scree test). **b** Distance between two merged clusters and the number of formed clusters

Strong negative anomalies of SLP were found for CP3 (n=329, 12.9 %) and slightly weaker for CP4 (n=469, 18.3 %) (Fig. 5c and d, respectively). CP3 shows a deep average low pressure over the adjacent Pacific Ocean and a northerly circulation associated with an increase in cyclonic activity (e.g., during the passage of extratropical frontal systems) that occurs more frequently in winter months (Fig. 6) after the weakening of the high pressures. CP4 shows a similar synoptic configuration of SLP and surface wind as CP3, but its more southern position and lower depth together with its more uniform annual occurrence (Fig. 6) suggest that CP4 corresponds to a low-pressure composite associated with the higher cyclonic activity in southern Chile. The northerly flow over central Chile that favors a warmer air advection appears to be more important for CP3 than for CP4.

The CPs of CP5 (n=168, 6.6 %) and CP6 (n=270, 10.5 %) (Fig. 5e and f, respectively) show large low-pressure systems such as in CP3 and CP4 but extend over the continent. These structures can be associated with the previously described CPs but in a subsequent phase with the cyclonic systems moving over Argentina. The associated circulations along the coast of central Chile change from a dominant negative meridional component for CP5 to a positive one for CP6, which modify their advective properties. The synoptic structure of CP5 reveals the orographic effect of the Andes on the SLP field, since the westerly flow can be perturbed by the presence of the highlands, which height descends from over 5,000 m in the north to ~2,000 m in the south; this effect was found initially by Lichtenstein (1989) and then discussed by other authors (e.g. Compagnucci and Salles 1997).

A high-pressure field in southern Chile extending over Argentina characterizes the CP7 (n=261, 10.3 %), which presents a high prevalence of occurrence in winter and

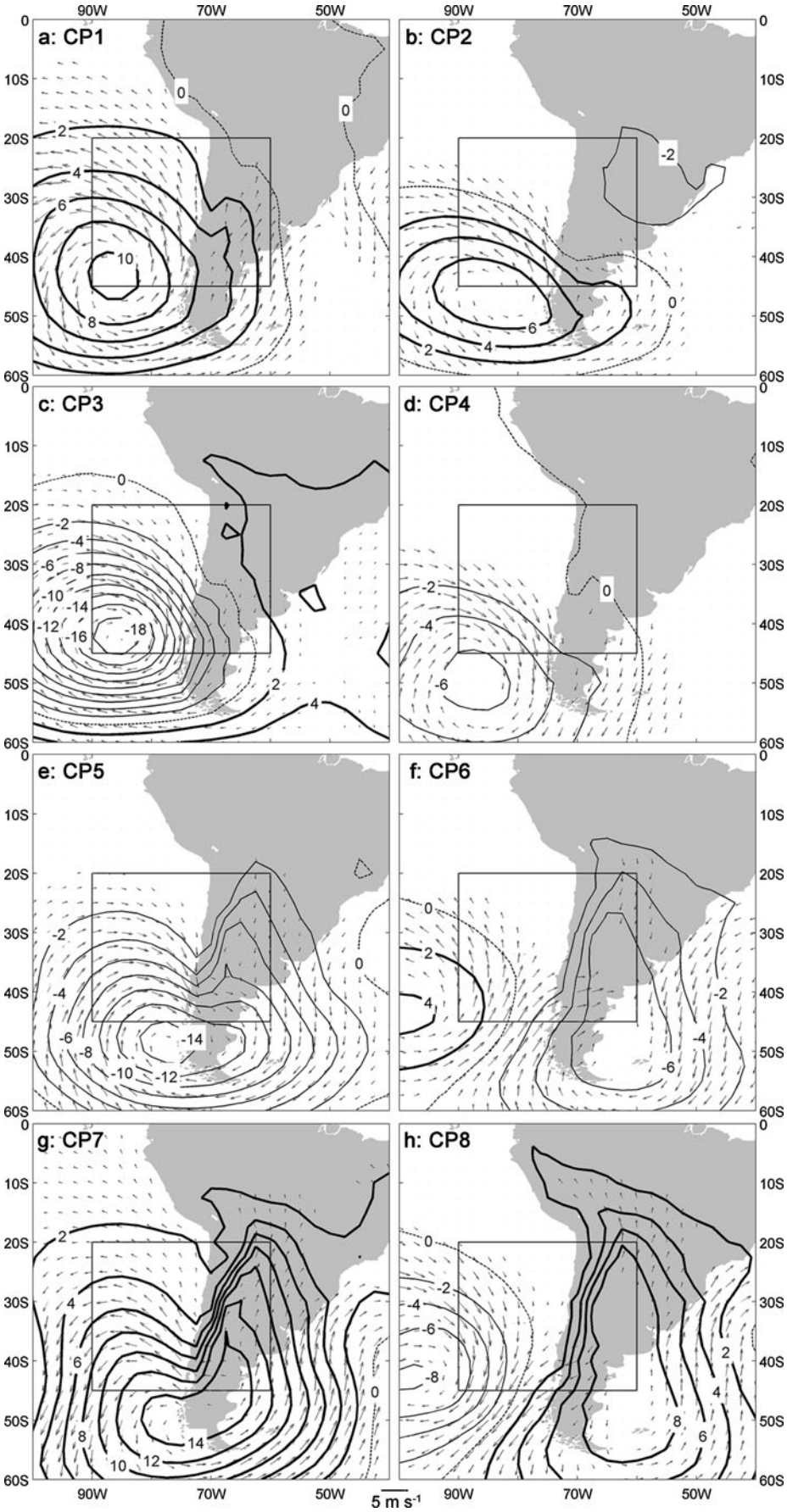

Fig. 5 Composites of sea level pressure (contoured every 2 hPa, *positive isobars in bold*) and wind vectors anomalies (meter per second; reference vector at the bottom) for the resulting circulation patterns. Only wind vectors with magnitude higher than 1 m s^{-1} are shown. The geographical window in which the classification was performed is also displayed (*interior rectangle*)

spring (Fig. 6). This corresponds to a migratory anticyclone crossing the southern Andes, generating a strong meridional pressure gradient over central Chile, which is associated with anomalies of easterly flow. Rutllant and Garreaud (2004) previously described this structure as responsible for intense downslope wind events in the valleys of central Chile, such as the Maipo Valley, locally known as *Raco* wind, generated by the geostrophic response to the surface pressure gradient. Also, this general synoptic pattern was identified as responsible of the development of coastal lows (or coastal troughs) over central Chile. Under such conditions, easterly winds depress the atmospheric boundary layer, and the adiabatically warmed air allows dominant clear skies and warm and dry days over the region (Garreaud et al. 2002; Garreaud and Rutllant 2003).

Finally, for CP8 (n=450, 17.6 %) a dipole of low and high SLP anomalies between the Pacific Ocean and the continent was revealed. An anomalous high-pressure area covering Argentina dominates the east side and a deep depression exists to the west, generating a strong zonal surface pressure gradient over Chile. A similar structure associated with cold conditions over Argentina was found by Escobar and Bischoff (1999). Given its occurrence during winter (Fig. 6), CP8 could be connected with some midlatitude cold high pressures described previously (CP7) but in a subsequent phase, thus producing a different surface circulation. The high-pressure system passing through southern Chile can reach the eastern part of the continent acting like a blocking system to lower pressures, which, in some cases, can be responsible for lower-than-normal temperatures over the continent (Pezza and Ambrizzi 2005; Müller and Berri 2007, 2012).

3.2 Circulation patterns (CPs) and minimum temperatures

The influence of the eight CPs on T_{min} in the Maipo and Casablanca valleys was investigated by calculating the deviations from the average temperature for the entire period 2001–2007 and the respective average value associated with each CP. The mean anomalies of T_{min} associated with the eight CPs are presented in Fig. 7.

Figure 7 shows that CP3 and CP5 have higher positive deviations in T_{min} (2.3 °C and 1.3 °C for the three weather stations on average, respectively), presenting significant differences for La Platina and Codigua stations. These low-pressure configurations associated to CP3 and CP5 are responsible for cloudy days and rainfall events, so that higher minimum AT_{min} are observed. Under these conditions, a less intense outgoing surface radiative flux and an enhanced incoming longwave radiation along with a large-scale northerly wind component can generate relatively high AT_{min} by reducing nocturnal cooling and bringing warmer air from lower latitudes. The more inland condition of La Platina station can explain the lower observed AT_{min} under weather conditions of CP5, since the northerly component is stronger over the adjacent ocean (Fig. 5e). For a complex mountainous terrain in Japan, Iijima and Shinoda (2002) found that the increase in seasonal (summer to autumn) intensity of nocturnal cooling was explained mainly by the reduction in incoming atmospheric radiation due to a lower air water content than by the decrease in outgoing longwave radiation due to the reduction in surface

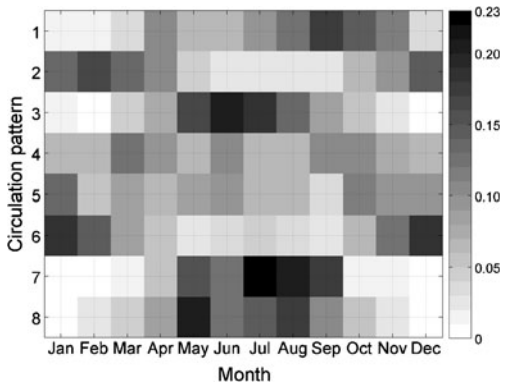

Fig. 6 Average monthly relative frequency of the eight circulation patterns. *Color bar* in fractional units

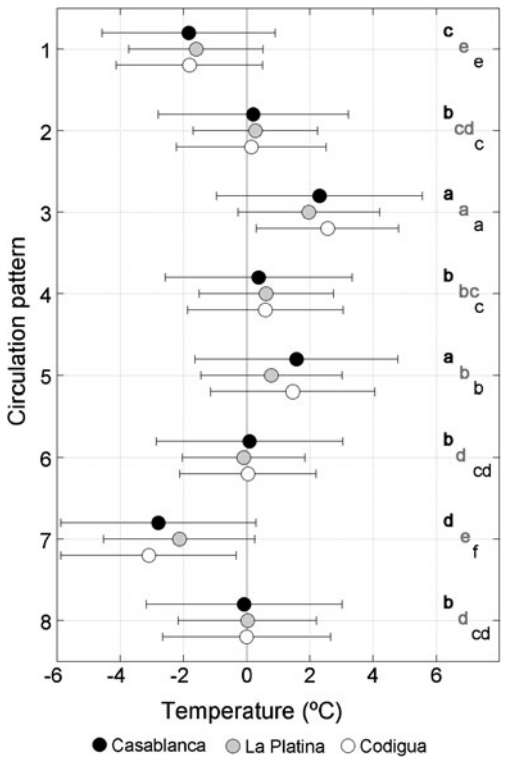

Fig. 7 Mean anomalies of minimum temperatures (*circles*) and standard deviation (*horizontal lines*) for the eight circulation patterns. *Different letters* denote significant differences among CPs for individual weather stations (for example, for Casablanca station, CP1 and CP2 shows significant differences, being AT_{min} of CP2 (**b**) higher than CP1 (**c**), and CP3 (**a**) with CP5 (**a**) are statistically equals) after a one-way ANOVA and Tukey's test ($p \leq 0.05$)

temperature, showing the high importance of cloudiness in determining surface temperature. Similar between stations, slightly positive and near to zero AT_{min} are associated with CP2, CP4, CP6, and CP8 (Fig. 7). These synoptic structures show very different configurations with weak surface wind anomalies and pressure gradients over the study area, so these structures are possibly more relevant over the southern part of the country, as observed at the bottom of the domain window used for the classification. Statistical differences are observed only in La Platina station for AT_{min} under these CPs.

CP1 and CP7 show negative anomalies of minimum temperatures (Fig. 7) (−1.7 °C and −2.7 °C for the three weather stations on average, respectively). The high pressures associated with CP1 generate cloudless skies that allow an enhanced surface cooling and cold air advection from higher latitudes in winter and spring months, in association with reinforcing of high-pressures (Fig. 2). In the classification of frost-related SLP patterns performed by Müller et al. (2003), high pressures were recognized as responsible for strong frost events over the wet Pampas region of Argentina.

CP7 showed the lowest AT_{min}, which are statistically different for Casablanca and Codigua stations in relation to others CPs and equal to CP1 for La Platina station. As mentioned in the previous section, the easterly and subsiding flow over central Chile generated by the strong meridional southern SLP gradient can produce clear skies and a very dry nocturnal boundary layer, leading to an enhanced radiative cooling. Surface air in low elevation zones of central valleys remains within a cold-air pool in nighttime and early morning, which results in low T_{min}. Interestingly, in the valleys of higher elevation and closer to the Andes, these *Raco* events induce anomalously warm nights (Rutllant and Garreaud 2004). The lower AT_{min} observed in Casablanca and Codigua could be related to their closer proximity to the sea than La Platina. The advection of cool marine air inland during the diurnal phase of the sea breeze circulation system induces a lowering of daily maximum temperatures in coastal stations, so that the overall large nocturnal cooling rates generated during the CP7 atmospheric conditions may allow lower nocturnal temperatures to be reached in areas closer to the sea as compared to more inland stations (e.g., Whiteman et al. 2004; Bonnardot et al. 2005). The influence of the Andes on this CP modifies its three-dimensional structure leading to a relative low pressure in the western part of the continent, which, in some cases, can lead to an increase in low cloudiness at the north of the low pressure (e.g., Garreaud et al. 2002; Vera et al. 2002). In a larger scale analysis, Müller and Berri (2007, 2012) found this dynamic structure responsible for persistent frosts over eastern South America, generating strong cold air advection by southerly wind anomalies.

Considering the different AT_{min} behavior showed by the eight CPs and its relevance for agricultural activities, the frost probability associated with each CP was calculated (Fig. 8). This was obtained by the simple ratio between the number of observed days with T_{min} lower than 0 °C and the total number of observations for the three weather stations. Consistent with their mean T_{min} differences (Fig. 3), the Casablanca station has, in general, the highest frost probabilities, followed by La Platina and Codigua stations. In CPs 2, 3, 4, 5, and 6, there is a frost probability close to zero, with only a few occurrences in the 7-year period that was analyzed. Among the eight CPs, CP7 stands out as the one with the highest frost probability (27.6 %, 21.2 %, and 14.7 % for Casablanca, La Platina, and Codigua, respectively), followed by CP1 (10.9 %, 9.4 %, and 3.3 %, respectively) and CP8 (7.8 %, 4.4 %, and 2.2 %, respectively). Finally, the annual distribution of CPs 1, CP7, and CP8 (Fig. 6) suggests that they can be responsible for winter and spring frosts that can cause damages to winter crops and early-bloom fruits trees and vineyards, a period in which many agricultural species are susceptible to injuries by low temperatures (Rodrigo 2000).

4 Conclusions

The influence of large-scale atmospheric structures on T_{min} over two Chilean agricultural valleys was analyzed for the period between January 2001 and December 2007. A statistical synoptic classification of SLP fields led to eight CPs with distinctive spatial and temporal characteristics. The mean anomalies of T_{min} (AT_{min}) for each CP were related to the different circulation types.

Although some CPs resulted in similar AT_{min}, it was possible to find a direct link between circulation and minimum temperatures. CPs occurring most frequently in summer months (CP2 and CP6) are not responsible for substantial variations in T_{min}, presenting anomalies of temperature near 0 °C. This is in agreement with the well-known southward

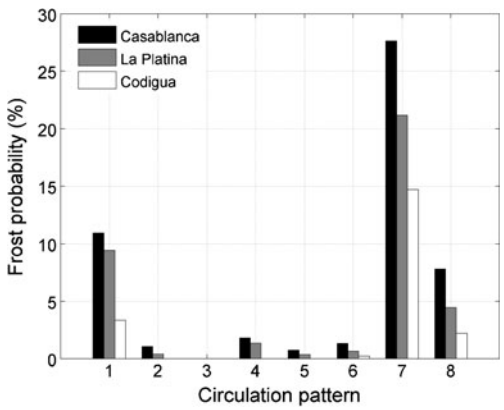

Fig. 8 Frost probability for the eight circulation patterns in Casablanca, La Platina, and Codigua

displacement of the subtropical anticyclone in the summer, which limits the arrival of perturbations from higher latitudes, therefore, reducing the synoptic-scale variability in central Chile. The relatively high average AT_{min} of CP2 and CP6 might not represent a major concern for agricultural crops grown in the Maipo and Casablanca valleys, given also that a very low frost risk can be linked to these pressure patterns.

During the cold season, a higher variability in CPs and temperatures was found. In general, positive (negative) SLP anomalies are related to negative (positive) AT_{min}. The higher anomalies of temperatures are associated with a deep low-pressure structure (CP3) centered over the Pacific Ocean, which could be related to rainfall events during the arrival of frontal systems to the region or to the presence of cyclonic activity that favors formation of clouds. Therefore, the arrival of warmer air from the north can be expected with an increase in AT_{min}. Conversely, the strengthening in high pressures allows a significant decrease in AT_{min}, with negative anomalies in the two valleys (CP1) with a larger occurrence in winter months. A migratory cold high was responsible for the lowest values of AT_{min} and a higher frost probability in CP7, which makes this structure the most important from an agricultural perspective, particularly for winter crops. Also, species such as fruit tree orchards or grapevines could be affected by springtime frosts under this synoptic structure.

Finally, a better understanding of the dynamics of large-scale atmospheric forcing on T_{min} in the Maipo and Casablanca valleys requires the study of other related factors and atmospheric variables at different spatial and temporal scales, such as radiative fluxes and air humidity. Numerical modeling of meso- and microscale aspects of the problem, such as local circulations, together with more detailed observations will be needed in future research in order to understand the finer scale variability of T_{min} in the valleys.

Acknowledgments The authors gratefully acknowledge the Dirección Meteorológica de Chile and the Centro Nacional del Medio Ambiente (CENMA) for providing the temperature data and to David A. Rahn (DGF-UCh) for the linguistic support. Authors are grateful to Gabriela V. Müller and an anonymous reviewer for valuable comments that improved the manuscript. The first author acknowledges the technological consortium Tecnovid S.A. (grant 05CTE02-12) for the financial support of this research, as part of a Master's degree in Meteorology and Climatology at the University of Chile.

References

Anderberg MR (1973) Cluster analysis for applications. Academic, New York

Ashworth EN (1992) Formation and spread of ice in plant tissues. Hortic Rev 13:215–255

Bonnardot V, Planchon O, Cautenet S (2005) Sea breeze development under an offshore synoptic wind in the South-Western Cape and implications for the Stellenbosch wine-producing area. Theor Appl Climatol 81:203–218

Cattell RB (1966) The scree test for the number of factors. Multivar Behav Res 1:245–278

Cellier P (1993) An operational model for predicting minimum temperatures near the soil surface under clear sky conditions. J Appl Meteorol 32:871–883

Clements CB, Whiteman CD, Horel JD (2003) Cold-air-pool structure and evolution in a mountain basin: Peter Sinks, Utah. J Appl Meteorol 42:752–768

Compagnucci RH, Salles MA (1997) Surface pressure patterns during the year over southern South America. Int J Climatol 17:635–653

ECMWF (2010) European Centre for Medium-Range Weather Forecasts, Reading, UK. Available at http://www.ecmwf.int/. Accessed Dec 2010

Escobar G, Bischoff S (1999) Meteorological situations associated with significant temperature falls in Buenos Aires: an application to the daily consumption of residential natural gas. Meteorol Appl 6:253–260

Falvey M, Garreaud R (2007) Wintertime precipitation episodes in central Chile: associated meteorological conditions and orographic influences. J Hydrometeorol 8:171–193

Faust M, Erez A, Rowland LJ, Wang SY, Norman HA (1997) Bud dormancy in perennial fruit trees: physiological basis for dormancy induction, maintenance and release. HortSci 32:623–629

Garreaud R (2000) Cold air incursions over subtropical South America: mean structure and dynamics. Mon Weather Rev 128:2544–2559

Garreaud R (2001) Subtropical cold surges: regional aspects and global distribution. Int J Climatol 21:1181–1197

Garreaud R, Aceituno P (2007) Atmospheric circulation and climatic variability. In: Veblen T, Young K, Orme A (eds) The physical geography of South America. Oxford University Press, USA, pp 45–59

Garreaud R, Rutllant J (2003) Coastal lows along the subtropical west coast of South America: numerical simulation of a typical case. Mon Weather Rev 131:891–908

Garreaud R, Rutllant J, Fuenzalida H (2002) Coastal lows along the sub-tropical west coast of South America: mean structure and evolution. Mon Weather Rev 130:75–88

Iijima Y, Shinoda M (2002) The influence of seasonally varying atmospheric characteristics on the intensity of nocturnal cooling in a high mountain hollow. J Appl Meteorol 41:734–743

Jackson DI, Lombard PB (1993) Environmental and management practices affecting grape composition and wine quality: a review. Am J Enol Viticult 4:409–430

Jiménez PA, González-Rouco JF, Montávez JP, Navarro J, García-Bustamante E, Valero F (2008) Surface wind regionalization in complex terrain. J Appl Meteorol Climatol 47:308–325

Jiménez PA, González-Rouco JF, Montávez JP, García-Bustamante E, Navarro J (2009) Climatology of wind patterns in the northeast of the Iberian Peninsula. Int J Climatol 29:501–525

Jordan DN, Smith WK (1995) Microclimate factors influencing the frequency and duration of growth season frost for sub-alpine plants. Agric For Meteorol 77:17–30

Lichtenstein E (1989) Some influences of the Andes Cordillera on the synoptic scale circulation. Preprints, Third Int. Conf. on Southern Hemisphere Meteorology and Oceanography, Buenos Aires, Argentina. Am Meteorol Soc 156–159

Marengo J, Cornejo A, Satymurty P, Nobre C, Sea W (1997) Cold surges in tropical and extratropical South America: the strong event in June 1994. Mon Weather Rev 125:2759–2786

Montecinos A, Aceituno P (2003) Seasonality of the ENSO-related rainfall variability in central Chile and associated circulation anomalies. J Climate 16:281–296

Montes C (2010) Minimum temperatures in the Casablanca Valley: analysis of its variability and comparison with results of the WRF model (in Spanish). M.Sc. thesis in Meteorology and Climatology,

University of Chile. Faculty of Physical and Mathematical Sciences, Santiago, p 107
Montes C, Perez-Quezada JF, Peña-Neira A, Tonietto J (2012) Climatic potential for viticulture in Central Chile. Aust J Grape Wine Res 18:20–28
Müller GV (2007) Patterns leading to extreme events in Argentina: partial and generalized frosts. Int J Climatol 27:1373–1387
Müller GV (2010) Temperature decreases in the extratropics of South America in response to a tropical forcing during the austral winter. Ann Geophys 28:1–9
Müller GV, Berri GJ (2007) Atmospheric circulation associated with persistent generalized frosts in central-southern South America. Mon Weather Rev 135:1268–1289
Müller GV, Berri GJ (2012) Atmospheric circulation associated with extreme generalized frosts persistence in central-southern South America. Clim Dyn 38:837–857
Müller GV, Compagnucci R, Nuñez MN, Salles A (2003) Surface circulation associated with frost in the wet Pampas. Int J Climatol 23:943–961
Müller GV, Ambrizzi T, Núñez MN (2005) Mean atmospheric circulation leading to generalized frosts in central southern South America. Theor Appl Climatol 82:95–112
Oke TR (1987) Boundary layer climates, 2nd edn. Routledge, New York
Pezza AB, Ambrizzi T (2005) Dynamical conditions and synoptic tracks associated with different types cold surge over tropical South America. Int J Climatol 25:215–241
Richman MB (1986) Rotation of principal components. J Climatol 6:293–335
Rodrigo J (2000) Spring frosts in deciduous fruit trees—morphological damage and flower hardiness. Sci Hortic 85:155–173
Romero R, Sumner G, Ramis C, Genovés A (1999) A classification of the atmospheric circulation patterns producing significant daily rainfall in the Spanish Mediterranean area. Int J Climatol 19:765–785
Rossi F, Facini O, Loreti S, Nardino M, Georgiadis T, Zinoni F (2002) Meteorological and micrometeorological applications to frost monitoring in northern Italy orchards. Phys Chem Earth 27:1077–1089
Rusticucci M (2012) Observed and simulated variability of extreme temperature events over South America. Atmos Res 106:1–17
Rutllant J, Garreaud R (2004) Episodes of strong flow down the western slope of the subtropical Andes. Mon Weather Rev 132:611–622
Satymurty P, Nobre C, Silva Dias PL (1998) South America. In: Karoly DJ, Vincent DG (eds) Meteorology of the Southern Hemisphere. Meteorological monographs (American Meteorological Society), Boston, pp 119–140
Snyder RL, de Melo-Abreu JP (2005) Frost protection: fundamentals, practice and economics, vol 1, Environment and Natural Resources Series. Food and Agriculture Organization of the United Nations (FAO), Rome
Trigo RM, Osborn TJ, Corte-Real JM (2002) The North Atlantic oscillation influence on Europe: climate impacts and associated physical mechanisms. Clim Res 20:9–17
Vera CS, Vigliarolo PK (2000) A diagnostic study of cold-air outbreaks over South America. Mon Weather Rev 128:3–24
Vera CS, Vigliarolo PK, Berbery EH (2002) Cold season waves over subtropical South America. Mon Weather Rev 130:684–699
Vosper SB, Brown AR (2008) Numerical simulations of sheltering in valleys: the formation of nighttime cold-air-pools. Bound-Lay Meteorol 127:429–448
Ward JH (1963) Hierarchical grouping to optimize an objective function. J Am Stat Assoc 58:236–244
Whiteman CD, Zhong S, Shaw WJ, Hubbe JM, Bian X (2001) Cold pools in the Columbia basin. Weather Forecast 16:432–447
Whiteman CD, Haiden T, Pospichal B, Eisenbach S, Steinacker R (2004) Minimum temperatures, diurnal temperature ranges, and temperature inversions in limestone sinkholes of different sizes and shapes. J Appl Meteorol 43:1224–1236
Wilks D (2006) Statistical methods in the atmospheric sciences, vol 59, 2nd edn, International Geophysics Series. Academic, New York
Zängl G (2005) Dynamical aspects of wintertime cold-air pools in an alpine valley system. Mon Weather Rev 133:2721–2740
Zhong S, Whiteman CD, Bian X, Shaw WJ, Hubbe JM (2001) Meteorological processes affecting the evolution of a wintertime cold air pool in the Columbia basin. Mon Weather Rev 129:2600–2613
Zhong S, Bian X, Whiteman CD (2003) Time-scale for cold-air pool break up by turbulent erosion. Meteorol Z 12:229–233